Didar and Hesarinejad
Chem. Biol. Technol. Agric. (2023) 10:67
https://doi.org/10.1186/s40538-023-00441-4

Chemical and Biological Technologies in Agriculture

RESEARCH

Open Access

Active packaging based on wheat germ protein isolate–*Malva sylvestris* leaf mucilage embedded with D-limonene nanoliposome: preparation and characterization

Zohreh Didar[1*] and Mohammad Ali Hesarinejad[2]

Abstract

Background The aim of this study is to prepare wheat germ protein/*Malva sylvestris* leaf mucilage (WGPI/MSLM) biocomposite layers embedded with D-limonene nanoliposomes (NLP). The effects of WGPI/MSLM ratio (0.4–2.5), NLP (0–3%), and glycerol content (35–50%, w/w based on WGPI weight) on water vapor permeability (WVP), thickness, antioxidant activity, mechanical properties, and solubility of the fabricated bio-nanocomposites were investigated through faced-centered central composite design.

Results Our results showed the effects of WGPI/MSLM ratio, glycerol content, and liposome content as well as the interaction between the ratio and NLP content on WVP was significant. The sample with 3% NLP and 35% glycerol and a ratio of 0.4 WGPI/MSLM had the lowest solubility. As the ratio of WGPI/MSLM increased, the value of tensile strength (TS) of the samples increased. The lowest elongation at break (26.21%) exhibited by film with 2.5 WGPI/MSLM, 35% glycerol, and no NLP. The highest antioxidant activity (58.6%) was observed in formulated films with 3% NLP, and a WGPI/MSLM ratio of 0.4. The optimal active film was obtained at a ratio of 0.4 WGPI/MSLM, 35% glycerol, and 3% NLP. The analysis confirmed the antibacterial activity of the optimal films against *Escherichia coli* and *Staphylococcus aureus*, as well as the larger contact angle of the optimal film compared to the control film and the greater roughness of the optimal film compared to the control sample.

Conclusions In conclusion, this study successfully produced active films of wheat germ protein/Malva sylvestris leaf mucilage embedded with D-Limonene nanoliposomes. The optimal active film exhibited low solubility, high tensile strength, high antioxidant activity, and antibacterial activity against *Escherichia coli* and *Staphylococcus aureus*.

Keywords Active film, Wheat germ protein isolate, *Malva sylvestris* leaf mucilage, D-limonene nanoliposome

*Correspondence:
Zohreh Didar
z_didar57@yahoo.com
Full list of author information is available at the end of the article

Graphical Abstract

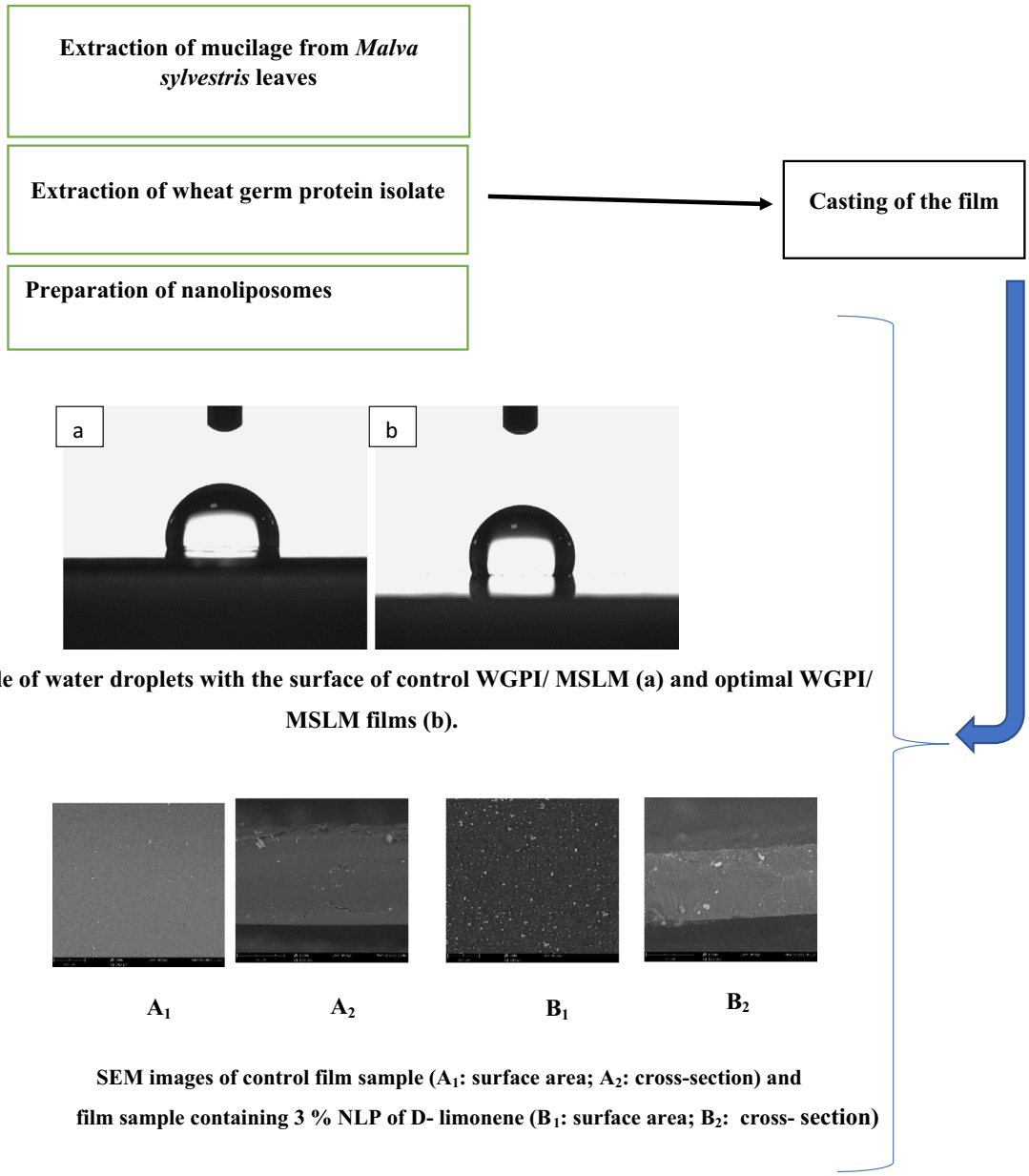

Introduction

Edible films are thin preformed layers of polymers applied to the surface of fresh fruits, vegetables and foods. They protect against adverse environmental conditions, act as physical barriers to mass transfer, and preserve food features, such as freshness, firmness, color, nutritional value and microbiological quality. Increasing consumer demand for fresh, high-quality, and sustainable foods has directed research toward the development of novel food preservation technologies using renewable and biodegradable materials [1] edible films and coatings are fabricated applying biodegradable, natural, and non-toxic biopolymers [2].

The three major biopolymers are carbohydrates, proteins, and lipids which naturally decompose without releasing toxic or dangerous components into the environment and, therefore, represent attractive alternatives to petroleum polymers [3]. In particular, protein-based edible films are of interest,

because they have higher nutritional value, better barrier properties and desirable mechanical properties than films made with carbohydrates or lipids [4, 5]. Several research efforts have developed edible films applying a wide range of proteins, such those based on milk protein-based [5], soy protein isolate [6], yellow pea (*Pisum sativum*) [7], faba bean protein isolate [8], corn starch/rock bean protein [9].

Mucilages as a novel resource for film forming have recently come into focus, e.g., chia seed mucilage [10], basil seed gum [11], and *Lallemantia peltata (L.)* seed gum [12] *Malva sylvestris*, usually referred to as common mallow. *M. sylvestris* is commonly used as a vegetable and medicinal plant in Iran, where it is named Panirak [13]. The leaves of *M. sylvestris* contain about 8.377 ± 0.38%, polysaccharides and showed strong scavenging activity for DPPH and hydroxyl radicals in vitro.

Wheat germ is a byproduct of wheat flour processing and composes of approximately 30% protein. Wheat germ protein mainly includes albumin (30.2%), globulin (18.9%), glutenin (0.3% ~ 0.37%), gliadin (14.0%), and 30.2% insoluble protein and other non-protein nitrogen, which is a potential plant protein resource [14].

The production of single films is simple, but the low physical efficiency and high sensitivity to heat are the major drawbacks of single films. Therefore, films made of a single material need to be combined with other materials to improve practical application [15]. Therefore, recently, more studies have focused on multicomponent and multilayer films, that can successfully change the efficiency and characteristics of the film [16].

Nowadays, the potential use of edible films or coating have been assessed to formulate edible coatings and films with specific functions such as carriers of antioxidants, flavoring and/or coloring agents, and antimicrobials to improve food safety and quality such as edible composite films of soy protein isolate and egg white composite edible films with incorporated cinnamaldehyde [17]. Limonene (4-isopropenyl-1-methylcyclohexene) ($C_{10}H_{16}$) is naturally synthesized in various plants. It is reported to have various functional properties, such as its potential as an antimicrobial, herbicidal, and antioxidant agent. Nonetheless, the application of limonene is subject to certain limitations related to its instability, fragility and volatility. If it is not protected from external factors (oxygen, light, and temperature), It might be easily degraded [18].

Encapsulation of essential oils has various advantages such as protection from drastic conditions such as light, oxygen, and heat [19] and prevention of its degradation or volatilization during film processing. Furthermore, they slow down the process of essential oil release from the film into the medium, which allows the activity to be maintained for a longer period of time [20].

There are several researches on fabrication of single edible films containing D-limonene [21, 22] but there are few studies on fabrication of multilayer films including D-limonene such as edible films of corn starch/rock bean protein loaded with D-limonene particles [9], and the incorporation of D-limonene nanoliposomes into a composite film of wheat germ protein/*Malva sylvestris* leaf mucilage has not been investigated. Based on these considerations, the rationale for this study is to produce active films active films of wheat germ protein/*Malva sylvestris* leaf mucilage embedded with D-limonene nanoliposomes. We also investigated the effects of WGPI/MSLM ratio, NLP content, and glycerol content on the water vapor permeability, thickness, antioxidant activity, mechanical properties and solubility of the fabricated bio-nanocomposites. A face-centered composite design (FCCD) was applied to determine the optimal treatment.

Materials and methods

Wheat germ flour was purchased from Golha Company. D-limonene was purchased from Abtin Chem CO.LTD. *Malva sylvestris* leaves were also purchased from a local market and authenticated by the Department of Systematic Plant Biology, Islamic Azad University, Neyshabur. Glycerol (> 99.0%), NaOH, HCl and other chemicals used in the present study were purchased from Sigma-Aldrich.

Extraction of wheat germ protein isolate (WGPI)

For the protein isolate, the method outlined by Acquah et al. was followed. Accordingly, wheat germ flours (1:10 w/v) were dispersed in 2 M NaOH at 25 °C for 4 h. Subsequently, centrifugation was performed at 18,000 g and 4 °C for 30 min. The supernatant was acidified to pH 4.5 with 2 M HCl for 4 h to precipitate the proteins, followed by centrifugation at 18,000 g and 4 °C for 30 min. The protein precipitates were neutralized with 2 M NaOH to pH 7.0. The protein isolate was frozen at − 80 °C for 24 h followed by freeze drying to yield the wheat germ protein isolate (WGPI) powder [7].

Extraction of mucilage from *Malva sylvestris* leaves (MSLM)

For the extraction of mucilage from *Malva sylvestris* leaves, the method outlined by Samavati et al. was followed. First, 2000 g of ground leaves were defatted and other impurities such as color agents and low molecular weight substances were removed with 80% EtOH at 60 °C for 2 h under reflux in Soxhlet's apparatus. The next step was to separate the organic solvent from the pretreated sample by centrifugation at 3000 × g for 10 min. 20 g of the dried pretreated samples were mixed with water under the following conditions (water temperature: 90 °C, extraction time: 4 h, the ratio of water to raw material: 21, and the number of extractions: 2). Thereafter,

they were filtered through a nylon cloth, concentrated and precipitated with ethanol (80%v/v). The precipitate was collected and finally air dried (at 50 °C) until it reached a constant weight [13].

Preparation of nanoliposomes

Nanoliposomes including limonene were prepared by the ethanol injection method of Sanei-Dehkordi et al. [23]. The lipid phase was first produced by dissolving lecithin (2.5% w/v), cholesterol (0.5%w/v), Tween 20 (1.0% w/v), and limonene (2% w/v), separately in absolute ethanol. Thereafter, one ml of each prepared solution was added dropwise to 4 ml of distilled water, and the mixtures were stirred (2000 rpm, room temperature) for 40 min [23].

Measurement of particle size and zeta potential of nanoliposomes

The particle size, zeta-potential and size distribution (polydispersity index) of nanoliposomes were measured by dynamic light scattering (DLS) using a Horiba SZ100 (Japan).

Casting of the film

Casting of the active films was done as method outlined by Acquah et al. and Ghasempour et al. with some modifications. Wheat germ protein isolate at a concentration of 4% (w/v) was dispersed in deionized water and stirred using a magnetic stirrer (10 min). The pH of the solution was adjusted to pH 8.0 with 0.1 M NaOH, followed by heating (75 °C for 30 min at 30 rpm). Then, the solution was maintained at room temperature for 30 min on a magnetic stirrer. MSLM was gently dissolving in distilled water (2%w/v) at 90 °C for 1 h, then kept at room temperature overnight. In this way, the ratios of WGPI to MSLM were set in the range of 0.4–2.5. Subsequently, the NLP were added at levels of 0–3%, and the mixture was subjected to 15 min of vigorous shaking at 40 ℃. Then, Glycerol (35–50%, w/v depending on the initial weight of WGPI) was added. The next stage included pouring solution (30 mL) onto sterile plastic Petri dishes (diameter, 90 mm) and dried at 25 °C for 72 h. After complete drying, dried films were conditioned in a humidity chamber at 25 ± 2 °C, and 50 ± 2% relative humidity [24, 24] before further analysis.

Thickness

The thickness of the prepared films was measured at ten different locations using a digital caliper with a resolution of 0.01 mm, and the average thickness was determined.

Tensile test

TS and elongation of the film were assessed according to the approach outlined by the Huang et al. [25] applying a texture analyzer (TA-XT PlusTM, Stable Micro Systems, England). Accordingly, a complete piece of film was cut into a specific diameter (4 mm×50 mm) and then fixed on the probe of the device while the initial gap set at 23 mm. The rate of stretching the film was 2 mm/s until cracked. The experiment was repeated three times for each film sample. TS (MPa) and EAB (%) were calculated by Eqs. (1) and (2):

$$\text{Ts (MPa)} = \frac{\text{F}}{\text{S}} \tag{1}$$

where F is the most tensile force (N), S is the cross-sectional area (mm^2) of the film sample:

$$\text{EAB (\%)} = \frac{L1 - L0}{L0} \times 100\% \tag{2}$$

where L_1 is the length of the film until crack (mm), and L_0 is the first length of the film (mm) [25]

Antioxidant capacity

The antioxidant capacity was determined by the 1,1-diphenyl-2-picrylhydrazyl (DPPH) free radical scavenging activity. First, 4 mg of the film was dissolved with 2 mL of ethanolic–DPPH (0.15 mol/L) and placed in a dark room for 30 min, filtered and the absorbance was determined at 517 nm [26]. The absorbance of the solution (methanolic–DPPH) was served as control. Results were reported as % of DPPH inhibition.

Water vapor permeability

In line with the method outlined by Ghasempour et al. (2022), the WVP of the samples was determined gravimetrically. First, a constant level of anhydrous $CaCl_2$ were weighed into cells and then sealed with film samples. Next, the RH in the desiccators was adjusted to 75% with saturated NaCl solution, and the weight changes of the cells were recorded every 6 h until a stable weight was reached. In addition, the weight gain of the system was measured to determine the water transfer across the film samples [24]. The WVP was calculated using the following equation:

$$\text{WVP} : \cdot \frac{\Delta m}{\Delta t \times A} \times \frac{x}{\Delta p}$$

where Δm/Δt represents the moisture uptake over time (g/s), X is the thickness average (mm), A is the area of the exposed film samples ($m.^2$), and Δp is the difference of water vapor pressure between inside and outside of the cell [27].

Water solubility

The determination of film solubility in water was carried out according to Attar et al. [24]. Briefly, the film samples were mixed with constant level of distilled water for 24 h at room temperature, after which the remaining samples

were dried and weighed. Water solubility was determined by the following equation:

$$\text{Water solubility (\%)} = \frac{Wi - Wf}{Wi} \times 100$$

where W_i is the initial weight of film, W_f is the final weight of film

Water contact angle assessment (WCA)

Static contact angle measurements were conducted on the films using a JIKAN instrument (CAG-20 SE) at ambient conditions by recording the side profiles of drops of deionized water (4 µl) placed on the film surface. The measurement was taken 2 s after the drop deposition to make sure stabilization of the drop and to minimize water absorption and evaporation. For each film, at least five drops were observed on different areas (both top and bottom), and contact angles were reported as average ± standard deviation [28].

FTIR

A FTIR spectrophotometer (Thermo, AVATAR model, USA) was applied to assess Fourier transform infrared (FTIR) spectra of the film samples in the range of 500–4000 cm^{-1} [29].

Antimicrobial activity

To evaluate the antimicrobial activity of films against *Staphylococcus aureus* (ATCC 43300) and *Escherichia coli O157: H7* (ATCC 35218) as typical Gram-positive and Gram-negative pathogenic microorganisms, respectively, the inhibition zone approach was carried out. For this reason, 10 mL of melted Brain Heart Infusion (BHI) agar was poured into plates to which 200 µl of the bacterial cultures (colony count of 10^8 CFU/mL) were added. The film discs were prepared and placed on it and incubated for 24 h at 37 °C in an incubator. After that, the plates were assessed for the zone of inhibition of the film discs. The diameter of the entire zone was measured and then subtracted from the diameter of the film disc [24].

Atomic force microscopy (AFM) analysis

According to Zuo et al. [27] the surface morphology of the films was assessed by atomic force microscopy (Ara pajuhesh, Brisk Model (Iran). Z-Scanner with 4µ maximum scan range and a resolution of 0.1 nm. The fundamental basis of AFM is to discover the forces between a cantilever and the sample surface (x–y plane), which are translated into a deflection of the cantilever according to the Hooke's law and displayed as a topographic image with constant scan size. Data acquisition and image processing are performed by Real-time 100 Mb/s compatible with Windows 10 and via independent software, respectively. Finally, the roughness of the film surface was presented as R_a, R_q, R_v, and R_p. R_a: arithmetical mean deviation of the roughness profile. R_q is the root mean square deviation of the roughness profile, R_p is the maximum peak height of the roughness profile, R_v is the maximum valley depth of the roughness profile [30].

SEM analysis

Square samples with diameter About 3 × 3 mm were cut from the composite film. The samples were imaged using an SEM instrument (Phenom Prox, Netherlands).

Experimental design and statistical analysis

A faced-centered central composite design (FCCD) was applied for determination the optimal magnitudes of the three independent variables, including WGPI/MSLM ratio (0.4–2.5% gum), glycerol content (depending on the initial weight of WGPI) (35–50%) and nanoliposome percentage (0–3%) coded at three levels (− 1, 0 and + 1). A total of twenty experiments (including seven replicates at the center point) were conducted. The data were analyzed using the Design-Expert software (version 13, Stat-Ease Corporation, Minneapolis, MN, The USA) by fitting the second-order polynomial model:

$$Y = \beta_0 + \beta_1 x_1 + \beta_2 x_2 + \beta_3 x_3 + \beta_{12} x_1 x_2 + \beta_{13} x_1 x_3 + \beta_{23} x_2 x_3 + \beta_{11} x_1^2 + \beta_{22} x_2^2 + \beta_{33} x_3^2$$

where Y is the response calculated by the model (Water vapor permeability, Solubility, Tensile strength, elongation, thickness and antioxidant activity); x_1, x_2, and x_3 are the independent variables; β_0 is the interception

Table 1 Variables and their levels in the central composite design

Factors: independent variables		Level used
x_1 = The ratios of WGPI to MSLM	0.4	2.5
x_2 = Glycerol (according to the starting WGPI weight) (%)	35	50
x_3 = Nanoliposome (%)	0	3
Responses	Goal	
WVP (10^{-11} g/m s Pa)	min	
Solubility (%)	min	
Tensile Strength (MPa)	max	
Elongation (%)	max	
Thickness (mm)	min	
Antioxidant activity (%)	max	

WGPI: Wheat germ protein isolate, MSLM: Mucilage of *Malva sylvestris* leaves

Table 2 Sequential model sum of squares analyzed for responses (WVP, Solubility, Tensile Strength, Elongation, Thickness and Antioxidant activity)

Source	Water vapor permeability (10^{-11} g/m s Pa)				Solubility (%)			
	df	Sum of squares	F value	Prob. F	df	Sum of squares	F value	Prob. F
Mean vs Total	1	893.78			1	25582.7		
Linear vs Mean	3	33.03	10.51	0.0005	3	686.39	20.63	< 0.0001
2FI vs Linear	3	7.42	3.44	0.0488	3	47.62	1.59	0.2398
Quadratic vs 2FI	3	5.77	5.37	0.0184	3	91.64	8	0.0052
Cubic vs Quadratic	4	0.85	0.4671	0.7592	4	25.67	3.07	0.1066
Residual	6	2.73			6	12.54		
Total	20	943.59			20	26446.57		
	Tensile Strength (MPa)				Elongation (%)			
Source	df	Sum of squares	F value	Prob. F	df	Sum of squares	F value	Prob. F
Mean vs Total	1	304.2			1	27202.69		
Linear vs Mean	3	19.2	9.03	0.001	3	521.83	11.28	0.0003
2FI vs Linear	3	3.89	2.27	0.1289	3	122.83	4.29	0.026
Quadratic vs 2FI	3	4.1	4.09	0.039	3	92.54	9.82	0.0025
Cubic vs Quadratic	4	0.632	0.3499	0.8356	4	16.73	1.71	0.2657
Residual	6	2.71			6	14.7		
Total	20	334.74			20	27971.32		
	Thickness (mm)				Antioxidant activity (%)			
source	df	Sum of squares	F value	Prob. F	df	Sum of squares	F value	Prob. F
Mean vs Total	1	0.5314			1	32385.15		
Linear vs Mean	3	0.0176	21.36	< 0.0001	3	3110.94	62.1	< 0.0001
2FI vs Linear	3	0.0019	3.41	0.05	3	21.63	0.3817	0.7679
Quadratic vs 2FI	3	0	0.05	0.9844	3	205.51	17.1	0.0003
Cubic vs Quadratic	4	0.0009	0.8537	0.5405	4	8.77	0.4208	0.7892
residual	6	0.0015			6	31.28		
Total	20	0.5534			20	35763.28		

coefficient;$\beta_{11}, \beta_{22} and \beta_{33}$ are the quadratic terms. β_{12}, β_{13}, and β_{23} are the interaction coefficients. Analysis of variance (ANOVA) of the results and the least significant difference test (LSD) was performed to determine significant differences ($p < 0.05$) in the active films. The sufficiency of the obtained models was investigated basis on the statistical parameters (R^2, adjusted-R^2, and coefficient of variation (CV)). The three-dimensional response surface analysis was performed for finding the optimal magnitude of parameters. The optimum treatment was assessed for structural, morphological and antibacterial properties. The variables and their magnitude in Central Composite Design are shown in Table. 1.

Results and discussion

DLS analyses of the nanoliposomes included limonene showed the particle size was in the range of 45–70 nm. This is in accordance of the measured particle size of nanoliposomes containing limonene reported by Sanaei-Dehkordi et al. [23]. Zeta potential was -45.21 ± 2 mV and PDI was equal to 0.45.

Experimental results

To fitting the variation of each response, the sum of the sequential squares, degree of freedom, F value, and p value of the models were evaluated for: Mean vs Total, Linear vs Mean, 2FI vs Linear, Quadratic vs 2FI, and Cubic vs Quadratic. The results pointed out that the quadratic model was the best-fitted model for all

Table 3 Analysis of variances (ANOVA) of RSM model corresponding to the responses (WVP, Solubility, Tensile Strength, Elongation, Thickness and Antioxidant activity)

Source	Mean	Std. Dev	CV	R^2	Adjusted R^2
WVP (10^{-11} g/m s Pa)	6.68	0.5983	8.95	0.9281	0.8635
Solubility (%)	35.77	1.95	5.47	0.9558	0.916
Tensile Strength (MPa)	3.9	0.578	14.82	0.8906	0.7921
Elongation (%)	36.88	1.77	4.81	0.9591	0.9223
Thickness (mm)	0.163	0.0138	8.44	0.8882	0.8366
Antioxidant activity (%)	40.24	2	4.97	0.9881	0.9775

responses except thickness which linear and 2FI were the best models fitted with it (Table 2). According to the ANOVA results, R^2 equal to 0.8882–0.9881 showing the high precision of the second-order polynomial model (Table 3). Furthermore, the lack of fit was insignificant for all the models at a 5% significance level, which imply that that the models were appropriate for prediction of the dependent variables (Table 4). The predicted equations for each variable are shown in Table 5.

Water vapor permeability (WVP)

Low WVP is a desirable characteristic of packaging materials as it leads to longer shelf life of food materials and reduces the spoilage rate of food materials [24]. The measured WVP was 3.1×10^{-11} to 9.1×10^{-11} g/m s Pa. The WVP values we determined are close to the reported WVP magnitude of edible films produced by zein and corn–wheat starch. The WVP determined in the Zuo et al. (2019) paper ranged from 8.89×10^{-11} g/m s Pa to 5.96×10^{-11} g/m s Pa [27]. The 3-D plot of WVP as a function of the ratio of WGPI/MSLM, glycerol content, and percentage of NLP added is shown in Fig. 1.

Our results imply that the influence of protein isolate to mucilage ratio, glycerol content, and liposome content as well as, the interaction of ratio and nanoliposome content on WVP was significant ($P<0.05$). The WVP capacity of the edible films increased with higher mucilage concentrations (lower protein isolate/mucilage ratio) but declined as film formulation loaded with nanoliposome (Fig. 1).

Polysaccharides increase water permeation despite their suitable barrier properties to gases [31]. The inclusion of lecithin (in nanoliposome structure) decreases WVP [32]. The addition of nanoliposomes to protein films can offer a plasticizing effect and decrease the solubility of the film, thereby lowering its WVP. The nanoliposomes, which are placed in the links between the polymer matrices, prevent gas and water diffusion across the film [33]. Similar trends were reported by Ghasempour et al. who reported that WVP declined as betanin nanoliposomes were added to Persian gum and whey protein bionanocomposite films, and the water vapor permeability of the film samples decreased [24].

In the present study, the magnitude of WVP, increased as the ratio of protein isolate to mucilage decreased. This observation is in alignment with Ghasempour et al. (2022) who reported that WVP increased with the addition of Persian gum to the whey films [24].

The addition of nanoliposomes declined the magnitude of the WVP of films (Fig. 1). Homayounpour et al. reported that the magnitude of WVP decreased with increasing nano liposomal caraway (*Carum carvi. L*) seed extract and attributed these observations to the presence of lipid components in the film structure which led to water barrier properties due to increasing swelling, resulting in water vapor resistance of the [34]. Therefore, the presence of nanoliposomes may provide a difficult path for the passage of water molecules.

Water solubility

According to data analysis, the interaction effect of NLP and WGPI/MSLM on solubility was significant ($P<0.05$). The sample containing 3% NLP and 35% glycerol and the ratio of WGPI/MSLM had the lowest solubility equal to 0.4. Solubility is concerning both the hydrophilic/hydrophobic ratio of liposomes and the number of free hydroxyl groups in the polymer matrix available for hydrogen bonding with the polymers [35]. According to the results, increasing the ratio of WGPI/MSLM led to an increase increasing the solubility of the films. In fact, solubility of the prepared films decreased with increasing mucilage content. These results might be concerning to the polymer constituents (soluble and insoluble fraction) and the reaction between the constituent in the film structure [36]. The addition of NLP to film structure resulted a decrease in the film solubility (Fig. 2). Nanoliposomes can bind with macromolecules, which restricts molecular movement and resulting in reducing of the film solubility [24].

This observation is in line with the finding of Puscaselu et al. who reported that the swelling index values

Table 4 ANOVA and regression coefficients of the response surface models

Response	Source	Sum of square	df	Mean square	Value F	Prob F
	Model	46.23	9	5.14	14.35	0.0001***
	x_1	9.03	1	9.03	25.21	0.0005***
	x_2	2.4	1	2.4	6.71	0.0270**
	x_3	21.61	1	21.61	60.37	< 0.0001***
	x_1x_2	0.08	1	0.08	0.2235	0.6465 ns
	x_1x_3					
	x_2x_3	7.22	1	7.22	20.17	0.0012***
	x_1x_2					
WVP (10^{-11} g/m s Pa)	x_2x_3	0.125	1	0.125	0.3492	0.5677 ns
	x_1^2	2.16	1	2.16	6.04	0.0339**
	x_2^2	0.0005	1	0.0005	0.0014	0.9706 ns
	x_3^2	0.2255	1	0.2255	0.63	0.4458 ns
	Residual	3.58	10	0.3579		
	Lack of Fit	2.03	5	0.4052		0.3889 ns
	Pure Error	1.55	5	0.3107		
	Model	825.66	9	91.74	24.01	< 0.0001***
	x_1	511.23	1	511.23	133.8	< 0.0001***
	x_2	54.76	1	54.76	14.33	0.0036***
	x_3	120.41	1	120.41	31.51	0.0002***
	x_1x_2	0.6612	1	0.6612	0.1731	0.6862 ns
	x_1x_3					
Solubility (%)	x_2x_3	43.71	1	43.71	11.44	0.0070***
	x_1x_2	3.25	1	3.25	0.8509	0.3780 ns
	x_2x_3					
	x_1^2	61.22	1	61.22	16.02	0.0025***
	x_2^2	3.75	1	3.75	0.9822	0.3450 ns
	x_3^2	21.28	1	21.28	5.57	0.0400**
	Residual	38.21	10	3.82		
	Lack of Fit	27.95	5	5.59	2.73	0.1476 ns
	Pure Error	10.26	5	2.05		
	Model	27.2	9	3.02	9.05	0.0010***
	x_1	2.21	1	2.21	6.61	0.0278**
	x_2	4.23	1	4.23	12.65	0.0052***
	x_3	12.77	1	12.77	38.22	0.0001***
	x_1x_2	0.845	1	0.845	2.53	0.1428 ns
	x_1x_3					
Tensile Strength (MPa)	x_2x_3	2.21	1	2.21	6.6	0.0279**
	x_1x_2	0.845	1	0.845	2.53	0.1428 ns
	x_2x_3					
	x_1^2	0.4009	1	0.4009	1.2	0.2990 ns
	x_2^2	0.0384	1	0.0384	0.115	0.7416 ns
	x_3^2	2.85	1	2.85	8.53	0.0153**
	Residual	3.34	10	0.3341		
	Lack of Fit	0.9661	5	0.1932	0.4068	0.8270 ns
	Pure Error	2.38	5	0.475		
	Model	737.21	9	81.91	26.07	< 0.0001***
	x_1	205.21	1	205.21	65.3	< 0.0001***
	x_2	19.6	1	19.6	6.24	0.0316**
	x_3	297.03	1	297.03	94.52	< 0.0001***

Table 4 (continued)

Response	Source	Sum of square	df	Mean square	Value F	Prob F
	x_1x_2	4.65	1	4.65	1.48	0.2517 ^{ns}
	x_1x_3					
Elongation (%)	x_2x_3	116.28	1	116.28	37	0.0001 ***
	x_1x_2	1.9	1	1.9	0.605	0.4547 ^{ns}
	x_2x_3					
	x_1^2	18.14	1	18.14	5.77	0.0372 **
	x_2^2	0.1309	1	0.1309	0.0417	0.8424 ^{ns}
	x_3^2	11.76	1	11.76	3.74	0.0818 ^{ns}
	Residual	31.42	10	3.14		
	Lack of Fit	19.61	5	3.92	1.66	0.2958 ^{ns}
	Pure Error	11.81	5	2.36		
	Model	0.0196	6	0.0033	17.21	< 0.0001 ***
	x_1	0.013	1	0.013	68.42	< 0.0001 ***
	x_2	0.0003	1	0.0003	1.32	0.2713 ^{ns}
	x_3	0.0044	1	0.0044	23.28	0.0003 ***
Thickness (mm)	x_1x_2	0.0006	1	0.0006	3.23	0.0954 ^{ns}
	x_1x_3	0.001	1	0.001	5.35	0.0378 **
	x_2x_3					
	x_1x_2	0.0003	1	0.0003	1.65	0.2214 ^{ns}
	x_2x_3					
	Residual	0.0025	13	0.0002		
	Lack of Fit	0.0011	8	0.0001	0.5293	0.7980 ^{ns}
	Pure Error	0.0013	5	0.0003		
	Model	3338.08	9	370.9	92.61	< 0.0001 ***
	x_1	26.24	1	26.24	6.55	0.0284 **
	x_2	1.16	1	1.16	0.2886	0.6028 ^{ns}
	x_3	3083.54	1	3083.54	769.94	< 0.0001 ***
	x_1x_2	1.81	1	1.81	0.4507	0.5172 ^{ns}
	x_1x_3					
Antioxidant activity (%)	x_2x_3	19.22	459930524115395001	19.22	4.8	0.0533 ^{ns}
	x_1x_2	0.605	1	0.605	0.1511	0.7057 ^{ns}
	x_2x_3					
	x_1^2	14.43	1	14.43	3.6	0.0869 ^{ns}
	x_2^2	0.1202	1	0.1202	0.03	0.8659 ^{ns}
	x_3^2	150.96	1	150.96	37.69	0.0001 ***
	Residual	40.05	10	4		
	Lack of Fit	13.34	5	2.67	0.4992	0.7680 ^{ns}
	Pure Error	26.71	5	5.34		

of sodium alginate, and agar are inversely proportional to the volume of essential oil (lemon, grapefruit, orange, cinnamon, clove, mint, ginger, eucalypt, and chamomile oils) added and attributed this observation to the strong hydrophobic nature of the essential oils [37]. The incorporation of hydrophobic components that do not solubilize in water protects the edible film's structure in water [38].

Mechanical properties

Tensile strength Tensile strength is a significant characteristic of films suitable for packaging purpose. The results showed that the impact of the of ratio of protein isolate to mucilage, glycerol content, and the amount of nanoliposomes on the TS of the samples were significant ($P < 0.05$) (Fig. 3). Notably, the maximum magnitude of TS belonged to the sample with the following formula: WGPI/

Table 5 Regression coefficients of the second-order polynomial model for the response variables

Response	Regression equation	Brief model	Fitted model
WVP (10^{-11} g/m s Pa)	$6.11 - 0.95x_1 + 0.49x_2 - 1.47x_3 - 0.95x_1x_3 + 0.8864{x_1}^2$	$R^2 = 0.9281$ Adjusted $R^2 = 0.8635$	Quadratic
Water Solubility (%)	$37.32 + 7.15x_1 + 2.34x_2 - 3.47x_3 + 2.34x_1x_3 - 4.72{x_1}^2 + 2.78{x_3}^2$	$R^2 = 0.9558$ Adjusted $R^2 = 0.9160$	Quadratic
Tensile Strength (MPa)	$4.28 + 0.47x_1 - 0.65x_2 + 1.13x_3 + 0.525x_1x_3 - 1.02{x_3}^2$	$R^2 = 0.8906$ Adjusted $R^2 = 0.7921$	Quadratic
Elongation (%)	$39.31 + 4.53x_1 + 1.40x_2 + 5.45x_3 + 3.81x_1x_3 - 2.57{x_1}^2$	$R^2 = 0.9591$ Adjusted $R^2 = 0.9223$	Quadratic
Thickness (mm)	$0.163 + 0.036x_1 + 0.021x_3 - 0.0113x_1x_3$	$R^2 = 0.8882$ Adjusted $R^2 = 0.8366$	Linear 2FI
Antioxidant activity (%)	$42.90 - 1.62x_1 + 17.56x_3 - 7.41{x_3}^2$	$R^2 = 0.9881$ Adjusted $R^2 = 0.9775$	Quadratic

MSLM: 2.5, glycerol: 35%, nanoliposome content: 3%. According to the results, the higher ratio of protein isolates to mucilage led to the higher TS value of the samples. Increasing the amount of added nanoliposomes resulted in increasing the TS in obtained films (Fig. 3). This finding is in agree with the results of Hashemi-Gahruie et al. 2017 who stated incorporation of (oregano and thyme) nano emulsion into methylcellulose-based films resulted in increasing TS of films [39] and this phenomenon could be interpreted by network strengthening occurred by great hydrogen bonding (dipole–dipole interactions) between polar groups, specially hydroxyl groups are in the polymer structure and polar head groups of surfactant molecules are at the interface of dispersed nanodroplets [38]. Ghasempour et al. (2022) stated that the TS of films had straight relation to the content of nanoliposomes and attributed this to the presence of lecithin in nanoliposome structure [24].

Elongation Our results indicated that all the parameters studied (ratio of protein isolate to mucilage, glycerol content, and the amount of nanoliposomes) had a significant impact on the percentage of elongation of the samples ($P < 0.05$). The film with a protein isolate to mucilage ratio = 2.5 and a glycerol content of 35% without a nanoliposome had lowest elongation (26.21%).

Increasing the ratio of WGPI/MSLM resulted in an increase in the magnitude of elongation percentage. In this context, Ghasempour et al. reported increasing the amount of Persian gum in nano-chitosan films resulted in a decrement in Young's modulus [24]. The inclusion of nanoliposomes into protein films can exert a plasticizing impact and improve the extensibility of the films [24] The results of the present study affirmed that an increase in the glycerol concentration led to an increase in the film elongation ($P < 0.05$), which is consistence with Abdolshahi et al. who reported that the magnitude of elongation of the edible film increased with the increase the glycerol content in the edible film formulation and attributed this observation to the decrease in rigidity and increase in flexibility of the films due to the glycerol present in the formulation [12]. As can be seen in Fig. 4, is obvious, further increased the elongation occurred as the content of nanoliposome in the active films increased. Homayounpour et al. reported that the magnitude of elongation increased in nanochitosan-based films containing higher nanoliposomal caraway (*Carum carvi. L*) seed extract and there was a significant difference between the control sample (without nanoliposome) and the samples containing nanoliposomes [34]. The ratio of protein isolates to mucilage in the film formulation also had a significant effect on the percentage of elongation ($P < 0.05$). As the content of wheat germ protein isolate was increased, the magnitude of the elongation increased.

Thickness

The obtained results revealed that among the three parameters studied, only the WGPI/MSLM ratio and NLP content had a significant effect on the thickness of the films ($P < 0.05$). Accordingly, the magnitude of thickness increased as wheat germ protein isolate/MSLM ratio increased. In fact, as the content of protein isolate in the film formulation was increased, the resulting film was thicker ($P < 0.05$) (Fig. 5). Similarly, Sogut et al. reported in edible film based on whey protein isolate and carrageenan, as the content of whey protein isolate increased, the thickness of the sample films also increased, as for the samples containing 75% and 50% whey protein isolate, the thickness was 126 ± 3 and 92 ± 7, respectively [40]. The sample with protein isolates to mucilage ratio of 0.4, 35% glycerol, and no added nanoliposomes had the lowest thickness (0.09 mm) and the highest thickness (0.21 mm) was observed for the sample with a ratio of 2.5 WGPI/MSLM, glycerol content = 35% and 3%

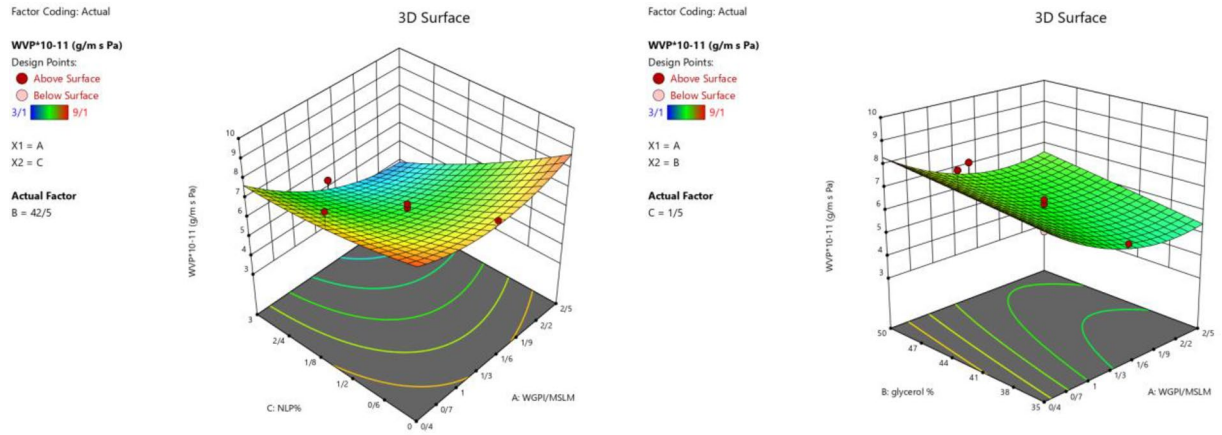

Fig. 1. 3D plot of the interaction impact of NLP and WGPI/MSLM ratio and glycerol content (%) (according to the starting WGPI weight) on the water vapor permeability in active film

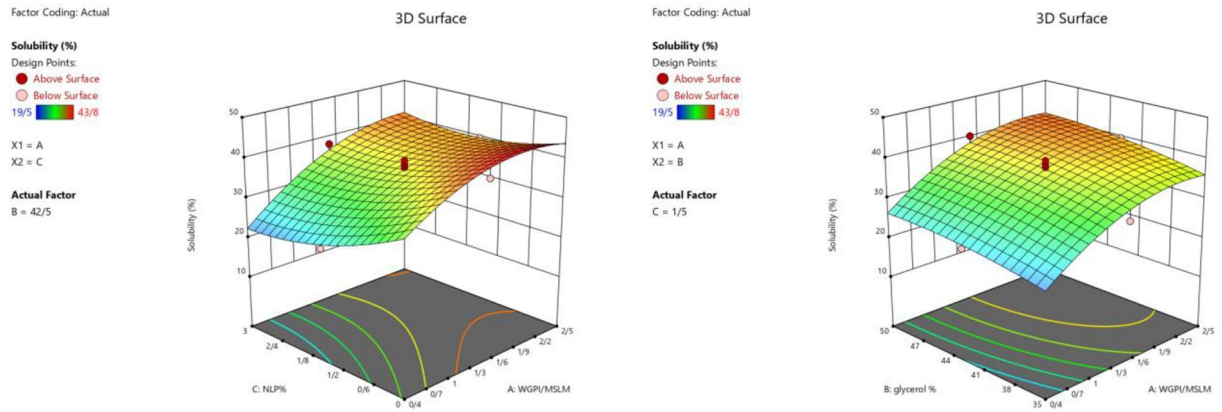

Fig. 2. 3D plot of the interaction impact of NLP and WGPI/MSLM ratio and glycerol content (%) (according to the starting WGPI weight) on the water solubility of films

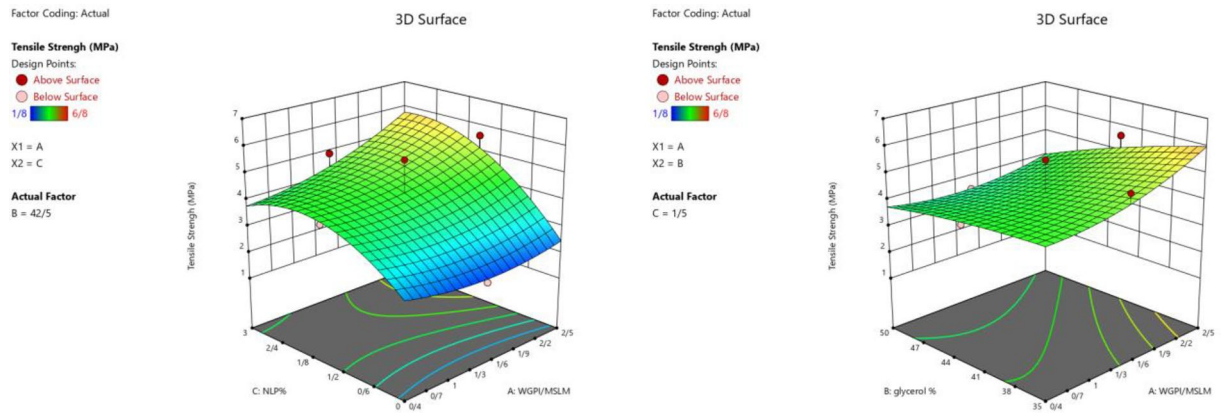

Fig. 3. 3D plot of the interaction impact of NLP and WGPI/MSLM ratio and glycerol content (%) (according to the starting WGPI weight) on the Tensile Strength of films

nanoliposome. The thickness of the films ranged from 0.09 to 0.21 mm. Incorporation of nanoliposomes into the films led to increases in film thickness. As the content of added nanoliposomes increased, the thickness of the films also increased, and there was a direct relationship between the content of nanoliposomes in the films and the thickness of the films. Najafi et al. reported that the thickness of pullulan films increased with the addition of saffron extract encapsulated in nanoliposomes, which was attributed to increase in dry matter in the films leading to increased thickness [41]. The difference in the thickness of the film samples might be due to the variation in their water holding capacity during the drying process [40].

Antioxidant activity

The results of antioxidant activity determination confirmed that both nanoliposome content and the protein isolate/mucilage ratio had significantly increased antioxidant capacity of the film ($P < 0.05$). The control sample without NLP also had antioxidant activity of 18.7–20.8%. This may be attributed to the antioxidant activity of *Malva sylvestris* polysaccharides. It has been reported that polysaccharides of *Malva sylvestris* have antioxidant activity. Samavati and Manoochehrizade reported that crude polysaccharides from the leaves of Malva sylvestris (MSLCP) exhibited remarkable DPPH radical scavenging activity, and DPPH radical scavenging effects increased with increasing concentrations of MSLCP [13]. The highest antioxidant activity was observed in formulated films containing 3% NLP, and the protein isolate/mucilage ratio was equal to 0.4 (58.6%).

According to the 3-D plot shown in Fig. 6, the antioxidant activity increased with increasing NLP concentration. The antioxidant property of limonene has been mentioned in several studies (Ibáñez et al.). Mahmoud (2017) reported that the antioxidant activity of *C. aurantifolia*, *C. limon*, and *C. paradisi* essential oils (40.16%, 57.20%, and 73.5% of limonene, respectively) occurred in a dose-dependent manner, with C. paradisi essential oil reaching values of 84.92% ± 0.5% and 92.45% ± 0.6% in the DPPH and β carotene linoleic acid assays reaching C. paradise essential oil values of 84.92% ± 0.5% and 92.45% ± 0.6% in the DPPH and β-carotene-linoleic acid assays, respectively [42].

Optimization

The response surface method (RSM) was applied for optimization, and the desirability function for each response was evaluated by numerical methods to obtain the overall desirability [43]. The responses to the optimal film are shown in Table 6. The optimal formulation for the active film was obtained with a WGPI/MSLM ratio of 0.4 and glycerol content of 35% and an NLP content of 3%. Experimental verification was conducted to further elucidate the reliability of the optimization outcomes and the results are shown in Table 6. Accordingly, the small deviation between the optimization outcomes and the experimental results for water vapor permeability, tensile strength, elongation, thickness, antioxidant activity, solubility, and sufficient desirability (0.826) indicate that the optimization results of this study are suitable. The desirability function is a strong tool to forecasting the optimal circumstances and in the present study the desirability was equal to 0.826 confirming the closeness to the target response (Table 7)

The optimal sample was investigated in terms of its structural (AFM, FTIR, WCA) and antimicrobial activity.

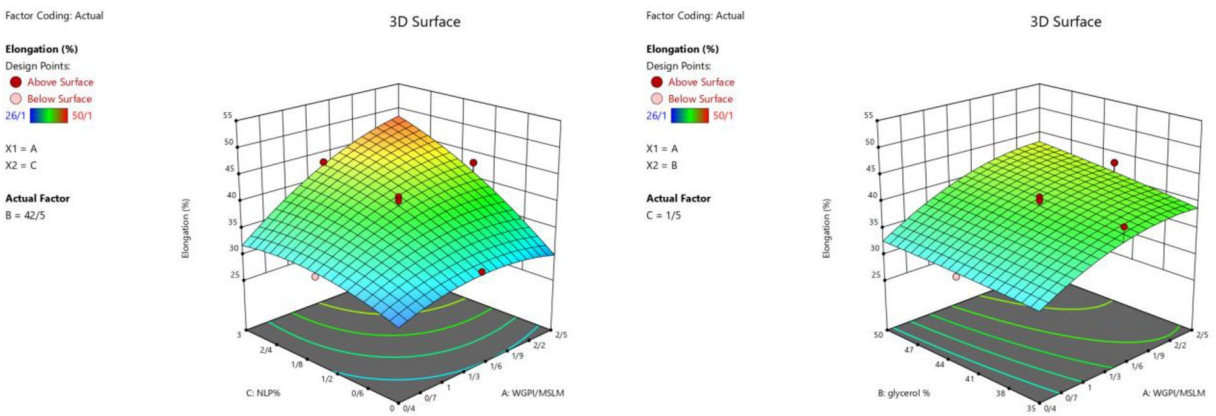

Fig. 4. 3D plot of the interaction impact of NLP and WGPI/MSLM ratio and glycerol content (%) (according to the starting WGPI weight) on the elongation (%) of films

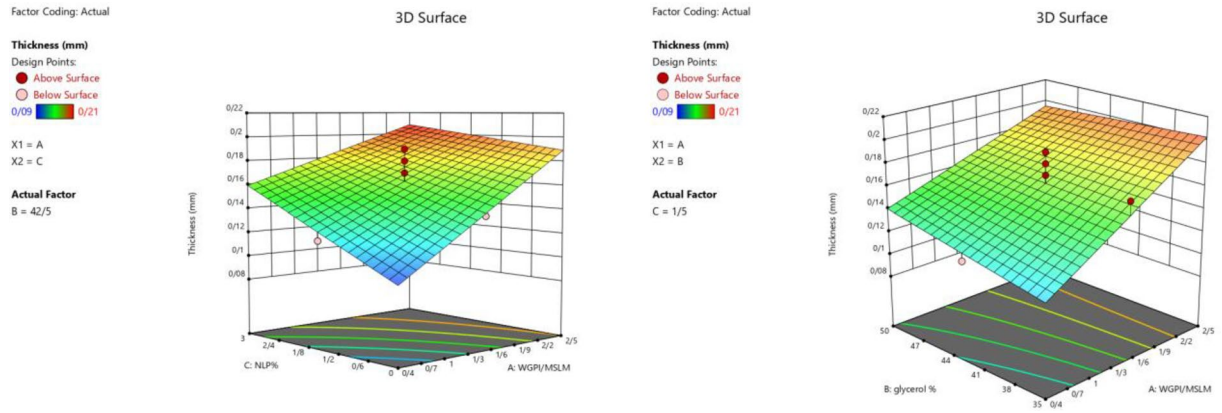

Fig. 5. 3D plot of the interaction impact of NLP and WGPI/MSLM ratio and glycerol content (%) (according to the starting WGPI weight) on the thickness of films

Antimicrobial activity

The examination for evaluating the antimicrobial properties was performed on the basis of determination of the zone of inhibition. The values of the zone of inhibition of the optimal film of WGPI/MSLM with NLP for *E. coli* O_{157}:H_7 and *S. aureus* were 2.1 and 2.42 mm, respectively. The larger the diameter of the inhibition zone, the higher the antimicrobial characteristics of the films. The optimally prepared film showed stronger activity against *S. aureus* (Gram-positive) than against *E. coli* (Gram-negative). This observation could be ascending to the structure of the outer membrane of E. coli; Gram-negative bacteria have a multilayered cell wall containing a peptidoglycan layer and an additional outer membrane [24] Chavosh et al. reported the antimicrobial activity of *Psyllium* seed gum films loaded with *Oliveria decumbens* essential oil against encapsulated in nanoliposomes against *E. coli and S. aureus*, with greater antibacterial activity against *S. aureus* [29]. The antimicrobial activity of limonene is reported by some researchers. Joshi et al. approves the lower mold incidence occurred in berries treated with the limonene–liposome compared to non-coated berries [44].

Water contact angle

The contact angle is an assessment of the affinity between the solvent and the surface of the material and is generally applied to evaluate of the wettability of the films. The contact angle of biopolymers varies from 0° (complete spreading of the liquid on the solid surface) to 180° (the unrealistic limit of absolute non-wetting [45]. The water contact angle of WGPI/MSLM films with and without NLP was measured by CAG-20 SE (JIKAN Co), and the results are shown in Fig. 7. The results showed that the contact angle of WGPI/MSLM film without NLP is 89.7 ± 1°, while it reaches 108 ± 1° in the case of NLP

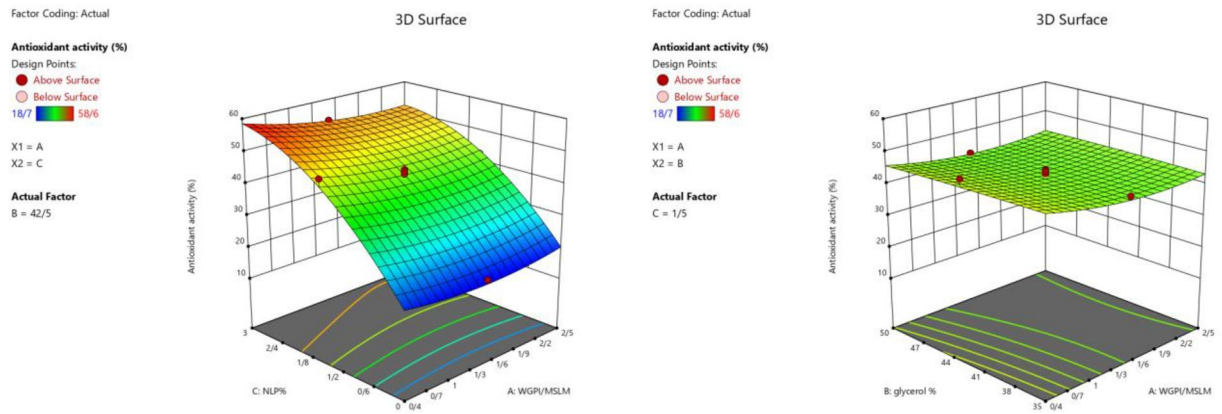

Fig. 6. 3D plot of the interaction impact of NLP and WGPI/MSLM ratio and glycerol content (%) (according to the starting WGPI weight) on antioxidant activity of films

Table 6 Comparison between theoretical and experimental results at the optimum condition predicted by the model

Parameter	Theoretical	Experimental	Goal	Lower limit	Upper limit
WGPI/MLM ratio	0.4	0.4	In range	0.4	2.5
NLP (%)	3	3	In range	0	3
Glycerol (%) (base on starting WGPI)	35	35	In range	35	50
WVP (10^{-11} g/m s Pa)	7.2	7.3	Min	3.1	9.1
TS (MPa)	4.6	4.6	Max	1.8	6.8
E (%)	31.8	31.7	Max	26.1	50.1
Thickness (mm)	0.12	0.12	Min	0.09	0.21
AA (%)	55.5	55.6	Max	18.7	58.6
Solubility (%)	19.6	19.5	Min	19.5	43.8

WGPI Wheat Germ Protein Isolate, *MSLM Malva sylvestris* leaves Mucilage, *NLP* Nanoliposomes, *TS* Tensile Strength, *E* Elongation, *AA* Antioxidant Activity

containing film. A low contact angle means the strong surface has hydrophilic characteristics, while a high contact angle is due to hydrophobic properties.

Table 7 FTIR spectrum of D-limonene, WGPI/MSLM films [51]

Sample	Wave number (cm^{-1})	Functional group
	886	C=C bending
Nanoliposome containing D-limonene	1250	C–O stretching
	1450	C–H bending
	1637	C=C stretching
	1670	C=O stretching
	1715	C=O stretching
	3345	O–H stretching
WGPI/MSLM film	1098	C–O stretching
	1248	C–O stretching
	1352	O–H bending
	1465	C–H bending
	1750	C=O stretching
	2929	C–H stretching
	3008	C–H stretching
	777	C–H bending
	885	C=C bending
	898	C–H bending
	987	C–H bending
WGPI/MSLM film containing NLP	1072	C–O stretching
	1140	C–O stretching
	1167	C–O stretching
	1201	C–O stretching
	1389	O–H bending
	1429	O–H bending
	1647	C=C stretching
	2899	C–H stretching
	3526	O–H stretching

When NLP were added to the active film, the WCA value increased, as shown in Fig. 7. The WCA value of the WGPI/MSLM film was comparable to that of mung bean starch/guar gum films [46]. The water contact point (θ) $\theta < 95$ implies to hydrophilic characteristics and $\theta > 95$ indicates hydrophobic properties [46]. It was observed that the addition of NLP into the film matrix led to higher contact angles between the water droplets and the surface of the films, making the films hydrophobic, with the hydrophobicity guided by the composition of the film [47]. These results agree with the WVP analyses, which revealed a homogeneous distribution and uniform NLP dispersion within the film matrix. This led to high contact angle values at the surfaces of the films. A similar behavior was found by Mendes et al. who observed increased contact angle values when higher amounts and hydrophobic compounds (cocoa butter) were incorporated into pectin films [48]. Similar results have been obtained in other studies, e.g., films prepared with the incorporation of *Oliveria decumbens* essential oil encapsulated in nanoliposomes in *Psyllium* seed gum films [29].

Ekrami et al. reported inclusion nanoliposomes of *Allium jesdianum Boiss*. into salep mucilage resulted in greater contact angle and explained that this finding might be due to the less availability of hydrophilic groups with increasing *Allium jesdianum Boiss* and reducing

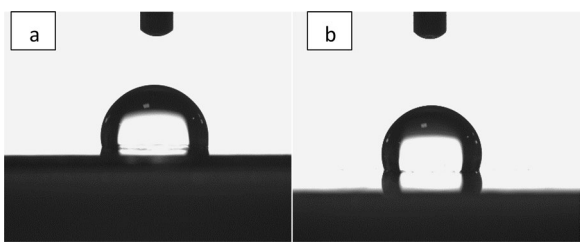

Fig. 7 Contact angle of water droplets with the surface of control WGPI/MSLM (**a**) and optimal WGPI/MSLM films (**b**)

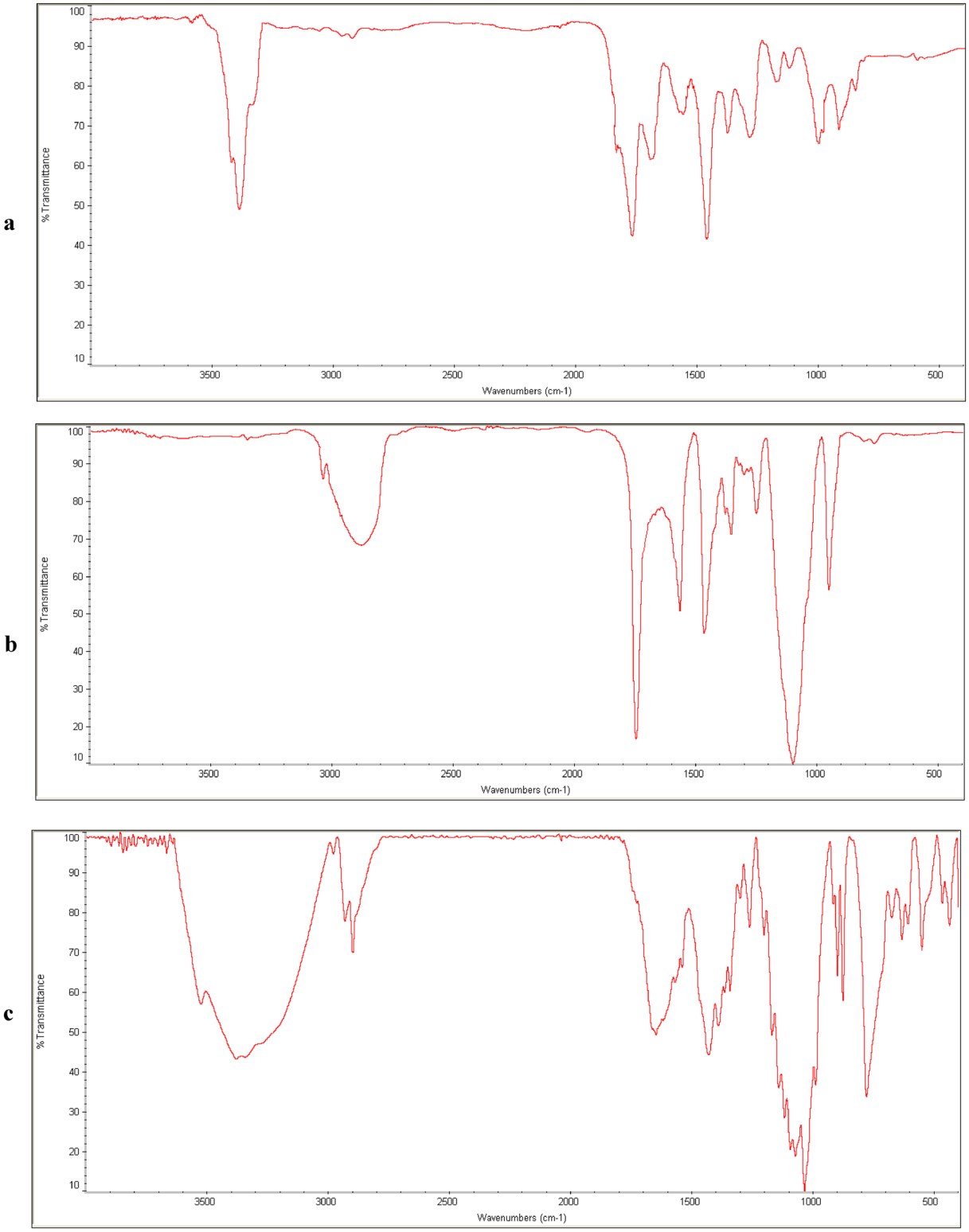

Fig. 8 FTIR of samples: nanoliposome of D-limonene (**a**); WGPI/MSLM film (**b**); WGPI/MSLM film containing NLP (**c**)

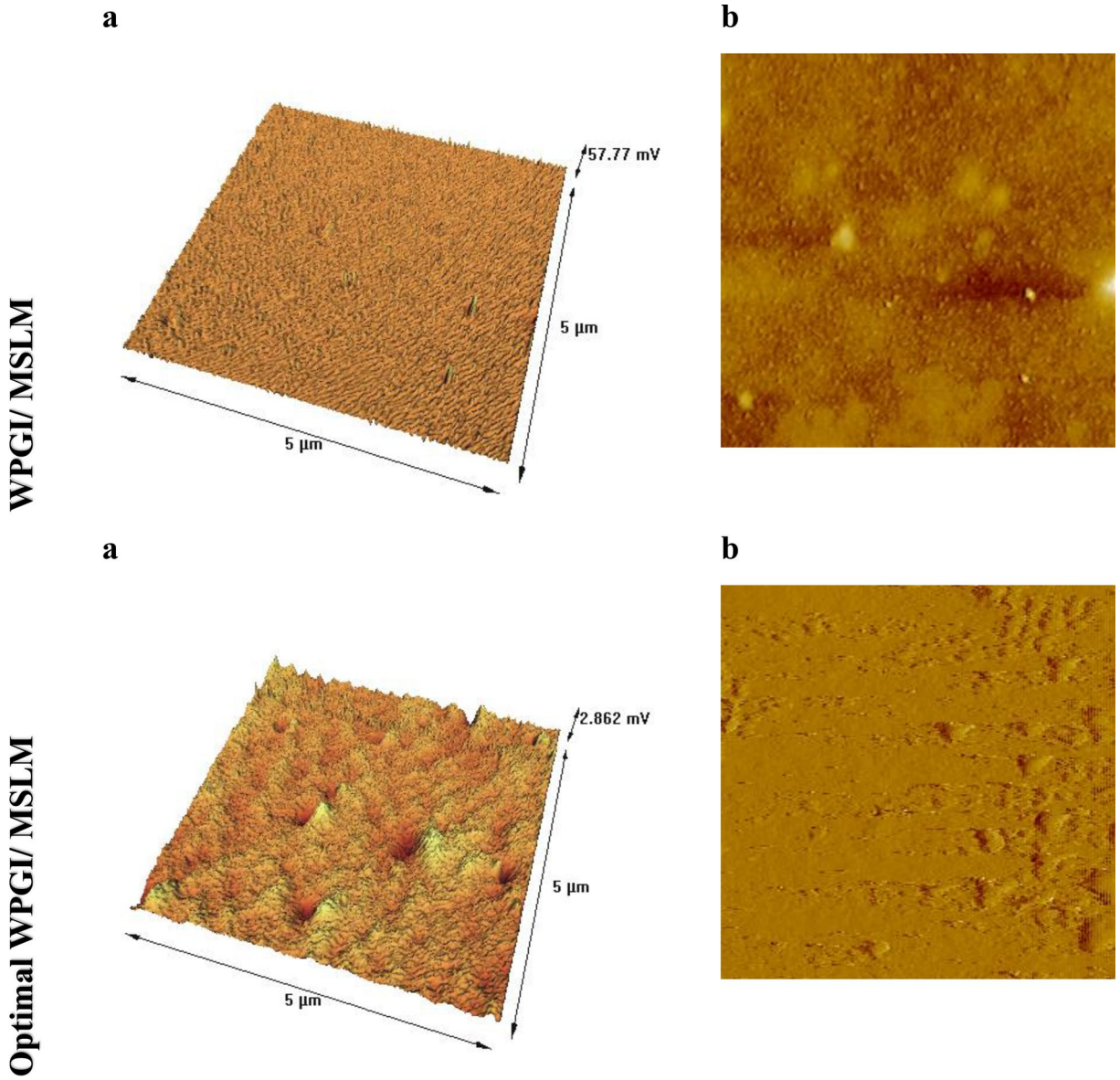

Fig. 9 Atomic force micrographs of surface topography 3-D (**a**) and 2-D (**b**) control WGPI/MSLM and optimal WGPI/MSLM

Table 8 Roughness parameters of WGPI/MSLM films

Sample	R_a (nm)	R_q (nm)	R_v (nm)	R_p (nm)
Control WGPI/MSLM	31.162[b]	36.862[b]	− 166.43[b]	83.038[b]
Optimal WGPI/MSLM	75.74[a]	87.83[a]	− 84.8273[a]	174.62[a]

the number of polar sites that may bind with water via hydrogen binding. The EOs non-polar molecules bound to the biopolymer molecules' surfaces are related to the increased hydrophobicity of the film samples [49].

FTIR

The FTIR spectrum of WGPI/MSLM film, nanoliposome of D-Limonene nanoliposomes, and WGPI/MSLM film containing NLP are depicted in Fig. 8. In the FTIR spectrum of limonene (Fig. 8a, the band at 3345 cm^{-1} is owing to the increasing the hydrogen bands between tween 20, OH of cholesterol, and carbonyl groups (C = O) of fatty acid esters in lecithin structure [23]. The peak that appeared at 1637 cm^{-1} could be attributed to the binding between lecithin and cholesterol, and the band at 961 cm^{-1} is ascending to $N(CH_3)_3$. The remarkable

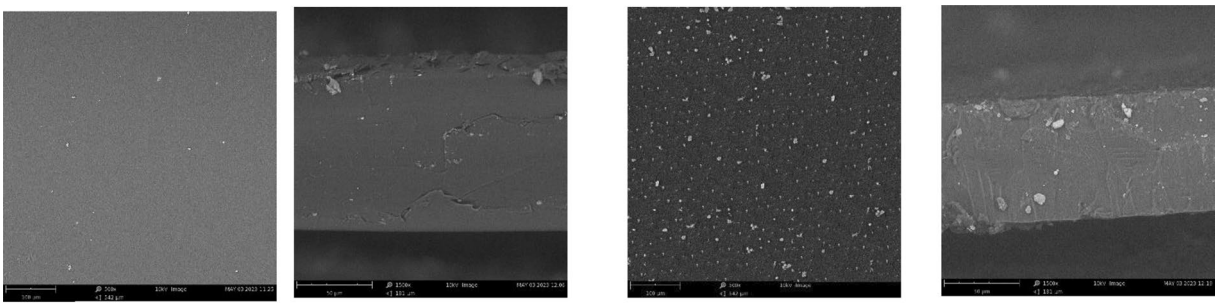

Fig. 10 SEM images of control film sample ($\mathbf{A}_1$: surface area; $\mathbf{A}_2$: cross section) and film sample containing 3% NLP of D limonene ($\mathbf{B}_1$: surface area; $\mathbf{B}_2$: cross section)

peak at 886 cm^{-1} is ascending to the terminal methylene group out of plane bending in limonene [23]. The bands appeared at 1670 and 1715 cm^{-1} could be assigned to C=O stretching [50].

FT-IR spectrum of WGPI/MSLM is shown in Fig. 8b. It is observed that the peaks at 1098 and cm^{-1} correspond to the C–O stretching. It should be noted the presence of a characteristic band at 1750 cm^{-1}corresponding to the stretching band of C=O. The intense bands at 1465, 2929, and 3008 cm^{-1} correspond to the C–H stretching. In the spectrum of WGPI/MSLM containing NLP (Fig. 8c), the peak at 2899 cm^{-1} is attributed to the C–H stretching in WGPI/MSLM and C–H of limonene. Two peaks appeared at 885 and 1647 cm^{-1} belonging to C=C stretching, the shape and position of the peaks affirmed that limonene was successfully encapsulated in active film. The bands at 777, 898, 987 and 2899 cm^{-1} can be assigned to C–H bending. The band at 1072, 1140, 1167, and 1201 cm^{-1} related to C–O stretching, and the bands observed at 1389, 1429, and 3526 cm^{-1}, are related to the O–H stretching. Table 3 shows the FTIR spectrum of D-limonene nanoliposomes and WGPI/MSLM films.

AFM

The atomic force microscopy (AFM) technique is a useful tool for evaluating the surface morphology of various films [27]. Figure 9 shows the 2-D and 3-D topography of the control and optimal films. The roughness (quantitative parameter) of the different films is depicted in Table 4. The WGPI/MSLM films with NLP had rougher surface than films without NLP (Fig. 9, Table 8). A similar value of R_a was reported by Beer-Lech et al. [30] for films made by adding psyllium husk to starch films. The R_q values of WGPI/MSLM films with and without NLP were 87.83 and 36.862, respectively, and the analysis showed a higher R_a magnitude for the film with NLP (Table 8). Thus, the control sample had a smoother surface than the film with NLP ($P<0.05$). According to the AFM images, the addition of NLP can increase the roughness of the film surface. In addition, the results of AFM analysis can be related to the WVP values. In general, WVP values decrease when R_a and R_q increase (53).

Different letters indicate significant differences between the values at the level of significance, $\alpha=0.05$.

SEM analysis

Figure 10 depicts SEM images of control sample and film sample containing 3% NLP. The compact morphologies obvious on both the surfaces and cross sections of the control film sample without NLPs, showing that wheat germ protein isolate-Malva sylvestris leaf mucilage has desirable film-forming ability which provide strong bonding during the film fabrication process. In the case of film containing NLP, the dense structures of film containing NLPs cross-sectional surface indicate desirable compatibility of constituents applied in film formulation. The film sample containing NLPs also shows uniform structure that could be attributed to the reaction between nanoliposomes and film matrix of films [29].

The impact of inclusion nanoliposomes into film formulation were reported in other studies. Chavoshi et al. reported addition of nanoliposomes of *O. decumbens* essential oil in the film formulation resulted in surface roughness in the structure of the films, which implies the presence of nanoliposomes in the film matrix [29].

Conclusion

The rationale for this study is to produce active films active films of wheat germ protein/*Malva sylvestris* leaf mucilage embedded with D-limonene nanoliposomes. We also investigated the effects of WGPI/MSLM ratio, NLP content, and glycerol content on the water vapor permeability, thickness, antioxidant activity, mechanical properties and solubility of the fabricated bio-nanocomposites. A face-centered composite design (FCCD)

was applied to determine the optimal treatment. Our results showed the effects of WGPI/MSLM ratio, glycerol content, and liposome content as well as the interaction between the ratio and NLP content on WVP was significant. The sample with 3% NLP and 35% glycerol and a ratio of 0.4 WGPI/MSLM had the lowest solubility. As the ratio of WGPI/MSLM increased, the value of tensile strength (TS) of the samples increased. The lowest elongation at break (26.21%) exhibited by film with 2.5 WGPI/MSLM, 35% glycerol, and no NLP. The highest antioxidant activity (58.6%) was observed in formulated films with 3% NLP, and a WGPI/MSLM ratio of 0.4. The optimal active film was obtained at a ratio of 0.4 WGPI/MSLM, 35% glycerol, and 3% NLP. The analysis confirmed the antibacterial activity of the optimal films against *Escherichia coli* and *Staphylococcus aureus*, as well as the larger contact angle of the optimal film compared to the control film and the greater roughness of the optimal film compared to the control sample.

Author contributions

Supervision, ZD; conceptualization, MAH; ZD; software, ZD; MAH; methodology, ZD; data curation, ZD; validation, ZD; MAH; formal analysis, ZD; writing—original draft, ZD; writing—review and editing, ZD; MAH.

Funding

The authors acknowledged the Iran High-Tech Laboratory Network for partial financial support of this research.

Availability of data and materials

Data are available upon request.

Declarations

Ethics approval and Consent to participate

All authors read and approved the final manuscript.

Consent for publication

All authors have read and agreed to the published version of the manuscript.

Competing interests

The authors declare no competing interests.

Author details

[1]Department of Food Science and Technology, Neyshabur Branch, Islamic Azad University, Neyshabur, Iran. [2]Department of Food Processing, Research Institute of Food Science and Technology (RIFST), Mashhad, Iran.

Received: 13 December 2022 Accepted: 12 July 2023
Published online: 01 August 2023

References

1. Avramescu SM, Butean C, Popa CV, Ortan A, Moraru I, Temocico G. Edible and functionalized films/coatings-performances and perspectives. Coatings. 2020;10(7):687.
2. Roy S, van Hai L, Kim HC, Zhai L, Kim J. Preparation and characterization of synthetic melanin-like nanoparticles reinforced chitosan nanocomposite films. Carbohydr Polym. 2020;231:115729.
3. Brodhagen M, Peyron M, Miles C, Inglis DA. Biodegradable plastic agricultural mulches and key features of microbial degradation. Appl Microbiol Biotechnol. 2015;99(3):1039.
4. Moghadam M, Salami M, Mohammadian M, Khodadadi M, Emam-Djomeh Z. Development of antioxidant edible films based on mung bean protein enriched with pomegranate peel. Food Hydrocoll. 2020;104:105735.
5. Fematt-flores GE, Aguiló-aguayo I, Marcos B, Camargo-olivas BA, Sánchez-vega R, Soto-caballero MC, et al. Milk protein-based edible films: influence on mechanical, hydrodynamic, optical and antioxidant properties. Coatings. 2022;12(2):196.
6. Zhang H, Wang L, Li H, Chi Y, Zhang H, Zhang X, et al. Changes in properties of soy protein isolate edible films stored at different temperatures: studies on water and glycerol migration. 2021. Foods. https://doi.org/10.3390/foods10081797.
7. Acquah C, Zhang Y, Dubé MA, Udenigwe CC. Formation and characterization of protein-based films from yellow pea (*Pisum sativum*) protein isolate and concentrate for edible applications. Curr Res Food Sci. 2020. https://doi.org/10.1016/j.crfs.2019.11.008.
8. Saremnezhad S, Azizi MH, Barzegar M, Abbasi S, Ahmadi E. Properties of a new edible film made of faba bean protein isolate. J Agri Sci Technol. 2011;13(2):181.
9. Luo S, Chen J, He J, Li H, Jia Q, Hossen MA, et al. Preparation of corn starch/rock bean protein edible film loaded with D-limonene particles and their application in glutinous rice cake preservation. Int J Biol Macromol. 2022;206:313.
10. Muñoz-tébar N, Carmona M, de Elguea-Culebras GO, Molina A, Berruga MI. Chia seed mucilage edible films with origanum vulgare and satureja montana essential oils: characterization and antifungal properties. Membranes. 2022;12(2):213.
11. Ansarian E, Aminzare M, Hassanzad Azar H, Mehrasbi MR, Bimakr M. Nanoemulsion-based basil seed gum edible film containing resveratrol and clove essential oil: In vitro antioxidant properties and its effect on oxidative stability and sensory characteristic of camel meat during refrigeration storage. Meat Sci. 2022;185:108716.
12. Abdolshahi A, Majd MH, Abdollahi M, Fatemizadeh S, Marvdashti LM. Edible film based on *Lallemantia peltata L.* seed gum: development and characterization. J Chem Health Risks. 2022;12(1):47.
13. Samavati V, Manoochehrizade A. Polysaccharide extraction from Malva sylvestris and its anti-oxidant activity. Int J Biol Macromol. 2013. https://doi.org/10.1016/j.ijbiomac.2013.04.050.
14. Tian S, Yu B, Du K, Li Y. Purification of wheat germ albumin hydrolysates by membrane separation and gel chromatography and evaluating their antioxidant activities. LWT. 2022. https://doi.org/10.1016/j.lwt.2022.113365.
15. Zhao R, Guan W, Zheng P, Tian F, Zhang Z, Sun Z, et al. Development of edible composite film based on chitosan nanoparticles and their application in packaging of fresh red sea bream fillets. Food Cont. 2022. https://doi.org/10.1016/j.foodcont.2021.108545.
16. Debeaufort F, Quezada-Gallo JA, Voilley A. Edible barriers: a solution to control water migration in foods. ACS Symp Series. 2000. https://doi.org/10.1021/bk-2000-0753.ch002.
17. Zhao X, Mu Y, Dong H, Zhang H, Zhang H, Chi Y, et al. Effect of cinnamaldehyde incorporation on the structural and physical properties, functional activity of soy protein isolate-egg white composite edible films. J Food Process Preserv. 2021. https://doi.org/10.1111/jfpp.15143.
18. Ibáñez MD, Sanchez-Ballester NM, Blázquez MA. Encapsulated limonene: a pleasant lemon-like aroma with promising application in the agri-food industry. A review. Molecules. 2020. https://doi.org/10.3390/molecules25112598.
19. Ruiz-Navajas Y, Viuda-Martos M, Sendra E, Perez-Alvarez JA, Fernández-López J. In vitro antibacterial and antioxidant properties of chitosan edible films incorporated with Thymus moroderi or Thymus piperella essential oils. Food Control. 2013. https://doi.org/10.1016/j.foodcont.2012.07.052.
20. Gómez-Estaca J, López-de-Dicastillo C, Hernández-Muñoz P, Catalá R, Gavara R. Advances in antioxidant active food packaging. Trends Food Sci Technol. 2014. https://doi.org/10.1016/j.tifs.2013.10.008.
21. Hou CY, Hazeena SH, Hsieh SL, Li BH, Chen MH, Wang PY, et al. Effect of D-Limonene nanoemulsion edible film on banana (Musa sapientum

Linn.) post-harvest preservation. Molecules. 2022. https://doi.org/10.3390/molecules27196157.
22. Miller KS, Upadhyaya SK, Krochta JM. Permeability of d-limonene in whey protein films. J Food Sci. 1998. https://doi.org/10.1111/j.1365-2621.1998.tb15718.x.
23. Sanei-Dehkordi A, Moemenbellah-Fard MD, Saffari M, Zarenezhad E, Osanloo M. Nanoliposomes containing limonene and limonene-rich essential oils as novel larvicides against malaria and filariasis mosquito vectors. BMC Complement Med Ther. 2022. https://doi.org/10.1186/s12906-022-03624-y.
24. Ghasempour Z, Khodaeivandi S, Ahangari H, Hamishehkar H, Amjadi S, Moghaddas Kia E, et al. Characterization and optimization of persian gum/whey protein bionanocomposite films containing betanin nanoliposomes for food packaging utilization. J Polym Environ. 2022. https://doi.org/10.1007/s10924-021-02367-0.
25. Huang X, Luo X, Liu L, Dong K, Yang R, Lin C, et al. Formation mechanism of egg white protein/κ-Carrageenan composite film and its application to oil packaging. Food Hydrocoll. 2020. https://doi.org/10.1016/j.foodhyd.2020.105780.
26. Lafarga T, Rodríguez-Roque MJ, Bobo G, Villaró S, Aguiló-Aguayo I. Effect of ultrasound processing on the bioaccessibility of phenolic compounds and antioxidant capacity of selected vegetables. Food Sci Biotechnol. 2019. https://doi.org/10.1007/s10068-019-00618-4.
27. Zuo G, Song X, Chen F, Shen Z. Physical and structural characterization of edible bilayer films made with zein and corn-wheat starch. J Saudi Soc Agric Sci. 2019. https://doi.org/10.1016/j.jssas.2017.09.005.
28. Siracusa V, Romani S, Gigli M, Mannozzi C, Cecchini JP, Tylewicz U, et al. Characterization of active edible films based on citral essential oil, alginate and pectin. Materials. 2018. https://doi.org/10.3390/ma11101980.
29. Chavoshi F, Didar Z, Vazifedoost M, Shahidi Noghabi M, Zendehdel A. Psyllium seed gum films loading Oliveria decumbens essential oil encapsulated in nanoliposomes: preparation and characterization. J Food Measure Charact. 2022;16(6):4318–30.
30. Beer-Lech K, Skic A, Skic K, Stropek Z, Arczewska M. Effect of psyllium husk addition on the structural and physical properties of biodegradable thermoplastic starch film. Materials. 2022;15:4459.
31. Khorram F, Ramezanian A, Hosseini SMH. Shellac, gelatin and Persian gum as alternative coating for orange fruit. Sci Hortic. 2017. https://doi.org/10.1016/j.scienta.2017.06.045.
32. Li X, Yang X, Deng H, Guo Y, Xue J. Gelatin films incorporated with thymol nanoemulsions: Physical properties and antimicrobial activities. Int J Biol Macromol. 2020;150:161–8.
33. Calva-Estrada SJ, Jiménez-Fernández M, Lugo-Cervantes E. Protein-based films: advances in the development of biomaterials applicable to food packaging. Food Eng Rev. 2019. https://doi.org/10.1007/s12393-019-09189-w.
34. Homayounpour P, Shariatifar N, Alizadeh-Sani M. Development of nanochitosan-based active packaging films containing free and nanoliposome caraway (Carum carvi. L) seed extract. Food Sci Nutr. 2021. https://doi.org/10.1002/fsn3.2025.
35. Marín-Peñalver D, Alemán A, Gómez-Guillén MC, Montero P. Carboxymethyl cellulose films containing nanoliposomes loaded with an angiotensin-converting enzyme inhibitory collagen hydrolysate. Food Hydrocoll. 2019. https://doi.org/10.1016/j.foodhyd.2019.04.009.
36. Emamverdian P, Moghaddas Kia E, Ghanbarzadeh B, Ghasempour Z. Characterization and optimization of complex coacervation between soluble fraction of Persian gum and gelatin. Colloids Surf A Physicochem Eng Asp. 2020. https://doi.org/10.1016/j.colsurfa.2020.125436.
37. Puscaselu RG, Lobiuc A, Gutt G. The future packaging of the food industry: the development and characterization of innovative biobased materials with essential oils added. Gels. 2022;8(8):505.
38. Kong I, Degraeve P, Pui LP. Polysaccharide-based edible films incorporated with essential oil nanoemulsions: physico-chemical, mechanical properties and its application in food preservation—a review. 2022. Foods. https://doi.org/10.3390/foods11040555.
39. Hashemi Gahruie H, Ziaee E, Eskandari MH, Hosseini SMH. Characterization of basil seed gum-based edible films incorporated with Zataria multiflora essential oil nanoemulsion. Carbohydr Polym. 2017;166:93–103.
40. Sogut E, Filiz BE, Seydim AC. Whey protein isolate- and carrageenan-based edible films as carriers of different probiotic bacteria. J Dairy Sci. 2022;105(6):4829–42.
41. Najafi Z, Kahn CJF, Bildik F, Arab-Tehrany E, Şahin-Yeşilçubuk N. Pullulan films loading saffron extract encapsulated in nanoliposomes; preparation and characterization. Int J Biol Macromol. 2021. https://doi.org/10.1016/j.ijbiomac.2021.07.175.
42. Mahmoud E. Essential oils of citrus fruit peels antioxidant, antibacterial and additive value as food preservative. J Food Dairy Sci. 2017. https://doi.org/10.2160/jfds.2017.37135.
43. Khosrow Shahi S, Didar Z, Hesarinejad MA, Vazifedoost M. Optimized pulsed electric field-assisted extraction of biosurfactants from Chubak (Acanthophyllum squarrosum) root and application in ice cream. J Sci Food Agric. 2021. https://doi.org/10.1002/jsfa.11000.
44. Joshi P, Becerra-Mora N, Vargas-Lizarazo AY, Kohli P, Fisher DJ, Choudhary R. Use of edible alginate and limonene-liposome coatings for shelf-life improvement of blackberries. Future Foods. 2021. https://doi.org/10.1016/j.fufo.2021.100091.
45. Jouki M, Mortazavi SA, Yazdi FT, Koocheki A. Optimization of extraction, antioxidant activity and functional properties of quince seed mucilage by RSM. Int J Biol Macromol. 2014. https://doi.org/10.1016/j.ijbiomac.2014.02.026.
46. Lee J-S, Lee E-s, Han J. Enhancement of the water-resistance properties of an edible film prepared from mung bean starch via the incorporation of sunflower seed oil. Sci Rep. 2020. https://doi.org/10.1038/s41598-020-70651-5.
47. Manrich A, Moreira FKV, Otoni CG, Lorevice MV, Martins MA, Mattoso LHC. Hydrophobic edible films made up of tomato cutin and pectin. Carbohydr Polym. 2017. https://doi.org/10.1016/j.carbpol.2017.01.075.
48. Mendes JF, Norcino LB, Manrich A, Pinheiro ACM, Oliveira JE, Mattoso LHC. Characterization of pectin films integrated with cocoa butter by continuous casting: physical, thermal and barrier properties. J Polym Environ. 2020. https://doi.org/10.1007/s10924-020-01829-1.
49. Ekrami M, Ekrami A, Hosseini MA, Emam-Djomeh Z. Characterization and optimization of salep mucilage bionanocomposite films containing allium jesdianum boiss nanoliposomes for antibacterial food packaging utilization. Molecules. 2022. https://doi.org/10.3390/molecules27207032.
50. IR Spectrum Table & Chart. Sigma Aldrich. IR Spectrum Table & Chart|Sigma-Aldrich. IR Spectrum Table & Chart. 2018.
51. Pan H, Jiang B, Chen J, Jin Z. Blend-modification of soy protein/lauric acid edible films using polysaccharides. Food Chem. 2014. https://doi.org/10.1016/j.foodchem.2013.11.075.

Publisher's Note